Extending the Reach of Short-Reach Optical Interconnects with DSP-Free Direct-Detection

Enrico Forestieri, *Member, IEEE*, Marco Secondini, *Member, IEEE*, Francesco Fresi, Gianluca Meloni, Luca Potì, *Member, IEEE*, and Fabio Cavaliere

***Abstract*—Coherent detection is the usual solution to achieve high bit rate transmission over long distance. However, it requires a local oscillator and energy consuming digital signal processing that make it not suitable for cost and energy sensitive interconnections and short haul links. In these applications, direct detection is the preferred solution and the main impairment is the chromatic dispersion of optical fibers. In theory, combined amplitude-phase shift (CAPS) codes are able to defeat any amount of chromatic dispersion. However, while they can be detected with a very simple direct detection receiver, their generation is not trivial. Their complexity grows with the order of the code which, in turn, increases with the chromatic dispersion. In this paper, the IQ-duobinary modulation scheme, a novel technique for approximating an order-3 CAPS code, is presented. Such a modulation scheme allows to bridge up to 18 km at a bit-rate of 50 Gb/s over a standard single mode fiber using a simple direct-detection receiver without the need of any digital signal processing technique.**

***Index Terms*—Optical fiber communication, optical interconnections, modulation formats, optical transmitters.**

I. Introduction

Short-reach optical interconnects are actively investigated in several application areas such as data center, baseband centralization in radio access networks (RANs), etc. In data centers, the need for increasing processing speed and capacity represents a major challenge for conventional solutions based on electrical switching, because of the inevitable increase in energy consumption and number of interconnections that follow [1]. Optical technologies based on dense wavelength division multiplexing (DWDM) could overcome both these limitations, thanks to the large bandwidth capacity of the optical fiber and to the low power consumption rate in optical switching. Therefore, a significant amount of research is being carried out to develop optical interconnects, networking technologies, and suitable modulation schemes for such applications [2]–[13].

Today, centralized RANs (CRANs) mainly rely on dedicated fiber connections between remote radio unit (RRU) nodes and baseband processing node. DWDM technologies can help to evolve the fronthaul network to face: *a)* the concurrent increase of bit rate and number of RRUs per area unit (respectively, 10 times to 100 times higher typical user data rate and 1000 times higher mobile data volume per geographical area, according to the 5G-PPP key performance indicators); and *b)* the consolidation of the number of baseband nodes in a fewer data center sites to save operational costs. The first aspect leads to an increase of the bit rate, up to 100 Gbit/s, the second aspect leads to an increase of the link distance.

Taking into account the maximum fiber propagation delay that most common fronthaul protocols can tolerate, typical distances that can be covered without optical amplification are up to 20 km. Nonlinear effects and polarization mode dispersion do not represent an issue for such short distances. Indeed, the major limiting transmission impairment is the chromatic dispersion, whose effects scale linearly with the distance and quadratically with the symbol rate, which should be in the order of 50 or 100 Gb/s to meet the capacity increase in the 5G transport network. In long-haul systems, this issue was traditionally addressed by deploying dispersion compensating fibers and, more recently, coherent detection and digital signal processing (DSP) [14]–[17]. However, as cost and power consumption at the receiver are important factors in short haul fronthaul and interconnection applications, coherent detection and DSP should be avoided, thus reducing the choice on the modulation format that can be used. Ideally, the adopted format should: *i)* allow for direct detection at the receiver, to decrease the optics cost by avoiding the local oscillator; *ii)* require minimal electronic processing at transmitter and receiver to save energy and cost; *iii)* allow for a low sensitivity receiver to achieve sufficient link budget with (or possibly without) optical amplification; *iv)* not require dispersion compensation up to 20 km. The simple on-off keying (OOK) format with direct detection is ruled out by the fourth mentioned constraint because it could only achieve a few kilometers at the considered bit rates without dispersion compensation. On the other hand, the use of multi-carrier modulation formats—such as orthogonal frequency-division multiplexing (OFDM) or its discrete multi-tone (DMT) variant—to reduce the impact of chromatic dispersion is better avoided because these techniques entail a significant increase of complexity, latency, and energy consumption [9].

Given the constraints listed above, the only way to combat chromatic dispersion seems to be using higher-order modulation formats, as they allow for a reduced symbol rate while maintaining the desired bit rate [18]. Indeed, unipolar four- and eight-level pulse amplitude modulation (PAM) formats

This work was supported in part by Ericsson.

Enrico Forestieri, Marco Secondini and Francesco Fresi are with TeCIP Institute, Scuola Superiore Sant'Anna, 56124 Pisa, Italy, and with National Laboratory of Photonic Networks, CNIT, 56124 Pisa, Italy. Gianluca Meloni and Luca Potì are with National Laboratory of Photonic Networks, CNIT, 56124 Pisa, Italy. Fabio Cavaliere is with Ericsson, 56124 Pisa, Italy.

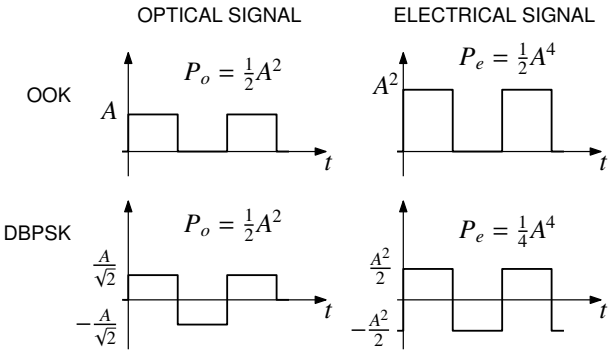

Fig. 1: OOK and DBPSK (lowpass equivalent) optical and electrical signals. The DBPSK electrical signal is polar because it is demodulated by an optical differential interferometer and detected by a balanced receiver.

(referred to as PAM-4 and PAM-8[1], respectively) have been proposed as candidate formats enabling a significant increase of the transmission distance compared to OOK [19], [20]. However, using unipolar higher-order formats may require more power compared to polar formats of same order to maintain the same spacing between levels. So, for example, PAM-4 should require more power compared to differential quadrature phase-shift keying (DQPSK), which also allows for direct detection through a differential interferometer that converts the phase modulation into amplitude modulation just prior photodetection [21]. Moreover, in the absence of optical amplifiers, noise is not involved in the phase-to-amplitude conversion process, such that there is no signal-noise beating and, at least when thermal noise dominates, DQPSK should have a clear advantage compared to PAM-4. Such a comparison was performed in [22] and it turns out that PAM-4 actually has an electrical power penalty of about 8 dB compared to DQPSK but almost no optical power penalty. That is to say, given the same optical power, the achieved bit error rate (BER) is the same in both cases but the generated electrical power is much less for DQPSK. This is better understood by comparing OOK and differential binary phase-shift keying (DBPSK). The corresponding (lowpass equivalent) optical and electrical signals are shown in Fig. 1 under the hypothesis of unit photodetectors' responsivity. As can be seen, given the same average optical power P_o, the electrical power P_e generated by DBPSK is half of the one generated by OOK but the BER is the same because the distance between signal levels is the same. In this case, as it is noiselessly demodulated in the optical domain, DBPSK has a 3 dB electrical power advantage over OOK but no optical power advantage.

Even taking into account that the capacitive coupling between the photodetector and the following circuitry blocks the direct-current (DC) bias, in the electrical domain DQPSK would have an advantage of about 4 dB over PAM-4 and would not require a digital-to-analog converter (DAC) at the transmitter and an analog-to-digital converter (ADC) at the receiver. Nevertheless, its receiver is possibly still too complex for short-reach interconnects applications.

As shown in [23], line coding (e.g., duobinary) does not allow to extend the reach when using multilevel formats. Indeed, signal spectrum compression is not, *per se*, the key factor to defeat chromatic dispersion. Rather, it is the combination of coding and proper pulse shaping that allows to increase the signal robustness, as demonstrated by the phase-shaped binary transmission (PSBT) technique and the combined amplitude-phase shift (CAPS) codes [24], [25].[2] It has been shown that an order-1 CAPS code has the same resilience to chromatic dispersion as DQPSK [26], while requiring (given a 1 dB optical power budget penalty) less optical power than DQPSK to bridge the same distance with a comparable spectral efficiency [22]. Moreover, CAPS codes of any order can be detected with the same receiver used for OOK [25]. However, their generation is not as simple, as an order-n coder has 2^n states and signals. Even the order-1 code uses signals that can put a burden on the electronics as they require a phase-shift just in the middle of a signaling interval. While an order-1 CAPS code can be very well approximated by narrow filtering a DBPSK signal [27], no simple way for generating or approximating higher-order codes is actually known. In this paper a relatively simple technique for generating an order-3 CAPS code is presented and the obtainable performance is compared to that of an actual order-3 code for transmitting at 50 Gb/s over a standard single mode fiber.

The paper is organized as follows. In Section II the CAPS codes are briefly reviewed and specific examples for an order-3 code are given; in Section III a transmitter structure able to approximate an order-3 code without using a DAC is introduced; in Section IV the performance obtainable by such approximation is compared to that of an actual order-3 code; finally, conclusions are drawn in Section V.

II. CAPS Coding

The main idea behind the CAPS codes is that a sufficiently dispersive fiber approximates a Fourier transformation, meaning that it turns an input pulse $s(t)$ with Fourier transform $S(f)$ and bandwidth B into an output pulse $v(t)$ whose envelope can be approximated as

$$|v(t)| \simeq \frac{1}{T\sqrt{\pi\gamma}} \left| S\Big(\frac{-t}{\pi\gamma T^2}\Big) \right|, \quad \text{for } \gamma(\pi BT)^2 \gg 1 \qquad (1)$$

where

$$\gamma = 2\lambda_0 R_b^2 D_a/\omega_0 \qquad (2)$$

λ_0 being the optical wavelength, $R_b = 1/T$ the bit rate, D_a the accumulated dispersion (usually given in ps/nm), and ω_0 the optical carrier angular frequency [25]. Moreover, this approximation becomes exact when the input pulse $s(t)$ is properly chirped [25]. This means that, for $\gamma' = \kappa\gamma$, replacing the input pulse $s(t)$ by $s'(t) = s(t/\kappa)/\sqrt{\kappa}$ will produce the same output pulse $v(t)$ (when properly chirped). This way, the same performance can be obtained irrespective of γ and

[1] In optics, when using direct-detection, PAM-M also refers to multilevel intensity modulation, where the information is instead associated to M different equispaced intensities of a supporting pulse.

[2] Note that CAPS coding is not related to carrierless amplitude modulation (CAP), which is a variant of quadrature amplitude modulation (QAM).

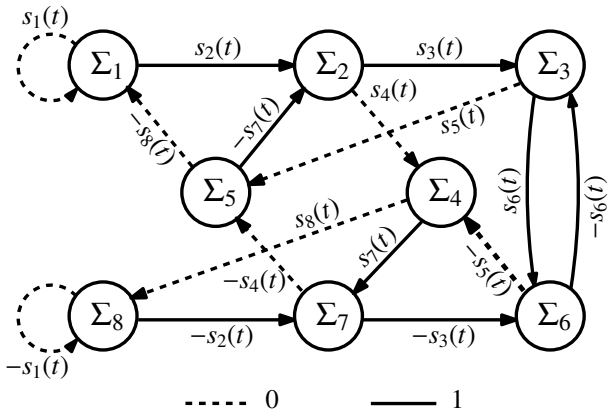

Fig. 2: State diagram of a CAPS-3 code.

thus any amount of chromatic dispersion can be (theoretically) defeated. As shown by (1), the most concentrated in frequency the input pulse, the less the broadening of the output pulse. Using a supporting pulse $g(t)$ larger than the signaling interval T and also differentially encoding the information bits to obtain a further reduction of bandwidth, the following PAM signal could be transmitted[3]

$$x(t) = \sum_{k=-\infty}^{\infty} w_k g(t - T - kT) \tag{3}$$

where

$$w_k = b_k - 0.5 \tag{4}$$

and the precoded symbols $b_k \in \{0, 1\}$ are obtained from the information symbols $u_k \in \{0, 1\}$ by precoding as

$$b_k = u_k + b_{k-1} \mod 2 \tag{5}$$

When $g(t)$ is chosen so that its in-phase and quadrature components are piecewise constant over a symbol time T,[4] the signal (3) can be produced by a coder whose state diagram and signals (of length T) are obtained as explained in [25]. Using a supporting pulse $g(t)$ of length $(n+1)T$ corresponds to an order-n CAPS code. For example, the state diagram of an order-3 code is as shown in Fig. 2 and the corresponding signals are given (for $i = 1, 2, \ldots, 8$) by

$$s_i(t) = \begin{cases} \sum_{k=0}^{3} (b_{i,k} - 0.5) g\big(t + (k-2)T\big), & 0 \le t \le T \\ 0 & \text{otherwise} \end{cases} \tag{6}$$

$$b_{i,k} = \left\lfloor \frac{i-1}{2^k} \right\rfloor \mod 2 \tag{7}$$

[3]The additional delay T in (3) is necessary only to make the sample $x(kT)$ correspond to w_k, because $g(t)$ is considered to be centered around the origin.

[4]Note that if $g(t)$ is chosen as a rectangular pulse of length $2T$ (with no quadrature component), then (3) would be a duobinary coded signal. In this case, in optics, (3) would be the driver signal of a Mach-Zehnder modulator (MZM) and the average value 0.5 may also not be removed as done in (4), so that $w_k = b_k$ and (3) would be a unipolar 3-level signal whose amplitude is adjusted to properly drive the MZM between two transmission maxima. Some MZMs allow to independently adjust the bias, so that (3) can also conveniently be zero-mean.

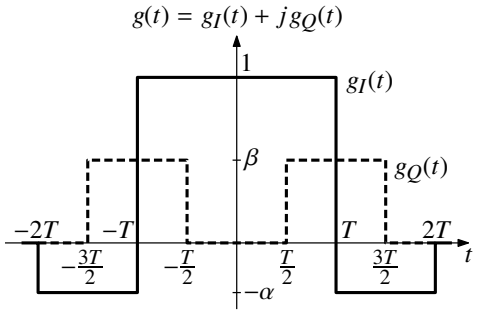

Fig. 3: Supporting pulse for a CAPS-3 code.

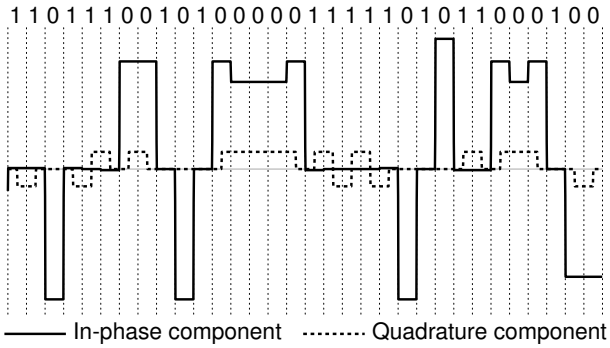

Fig. 4: CAPS-3 signal for $\alpha = 0.1$ and $\beta = 0.4$. Here the intensity of the signal components is represented, but with the sign of the corresponding electrical field.

The pulse $g(t)$ should have length $4T$ and its in-phase and quadrature components chosen in order to approximate the required chirp that makes (1) an exact relation. From a purely theoretical point of view, the best shape of $|g(t)|$ should be related to that of a prolate spheroidal waveform (most similar to a Gaussian shape), and thus the in-phase and quadrature components of $g(t)$ and the employed filters should also be chosen such that to approximate this shape [25]. A possible $g(t)$ is shown in Fig. 3, where the parameters α and β can be tailored to optimize the performance for different amounts of accumulated dispersion.

An example of the signal generated by a CAPS-3 code is shown in Fig. 4 for the given binary information sequence. In order to show the effect of the code, the intensity of each signal component is represented with the sign of the corresponding electrical field. The eye diagram obtained after propagating such signal through a standard single mode fiber at 50 Gb/s, tight filtering and photodetection is instead shown in Fig. 5 for three different fiber lengths, namely 0 km (back-to-back), 6 km, and 15 km. The eye diagrams on the right side correspond to the case in which only the in-phase component is transmitted. As can be seen, it is the quadrature component that allows to keep the eye open until well after 15 km.

The effectiveness of the CAPS-3 code has been experimentally demonstrated in [28] using a DAC for implementing the code through its 8-state diagram and signals (Fig. 2). It was found that the transmission distance can be increased by a factor of 4 and 1.5 in comparison to OOK and PAM-4, respectively. However, in order to be suitable for short-reach optical

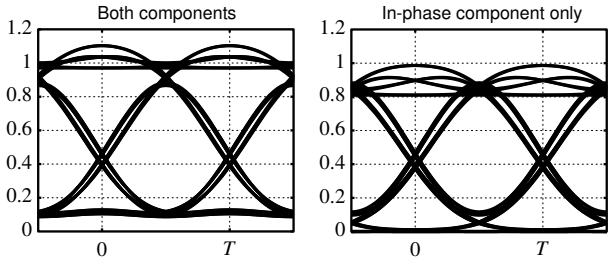

(a) Back-to-back

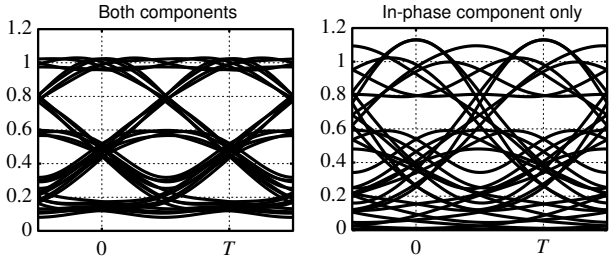

(b) After 6 km

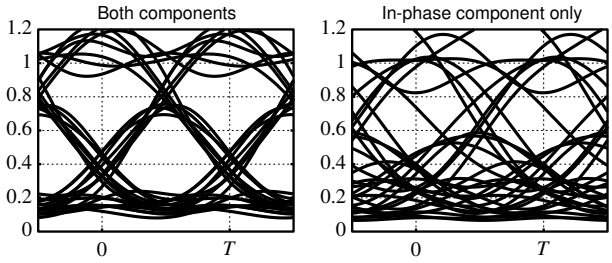

(c) After 15 km

Fig. 5: Eye diagrams of the CAPS-3 signal in Fig. 4 after filtering and photodetection. Only the in-phase component was transmitted for the diagrams on the right side.

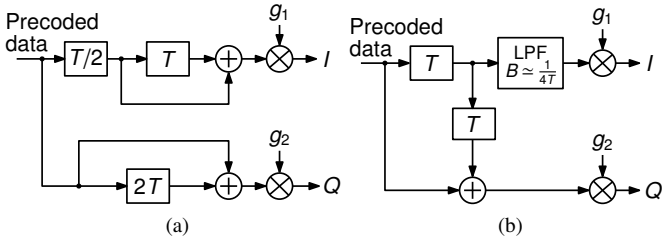

Fig. 6: Block diagrams for the generation of in-phase (I) and quadrature (Q) components. The duobinary in-phase component is ideal in (a) and obtained by filtering in (b).

interconnects applications, a much simpler implementation is required, preferably without the use of a DAC. In the following it will be shown that CAPS-3 coding can be implemented by using a transmitter whose complexity is comparable to that of a DQPSK transmitter, while still allowing for using an OOK receiver. Here we only deal with theoretical aspects, deferring experimental results (to be still obtained) to a later publication.

III. Approximating the CAPS-3 Code

As evident from Fig. 4, given $\alpha = 0.1$ and $\beta = 0.4$ (which is a good choice, as shown in the following), the in-phase component is very similar to a duobinary coded signal, and indeed it would be a duobinary signal for $\alpha = 0$. Thus, starting with non-return-to-zero (NRZ) pulses $p(t)$ of length T, we could approximate the signal (3) as shown in Fig. 6a, where the gains g_1 and g_2 are to be properly chosen (in this case, with reference to Fig. 3, it has to be $g_2 = \beta g_1$). However, the $T/2$ delay may be hard to implement, because it would require a clock at double the bit-rate in a digital implementation or a precision increasing with the bit-rate in an analog one. We can solve this issue by noting that the Fourier transform of $p(t)+p(t-T)$ is equal to $2e^{-j\pi fT}P(f)\cos\pi fT$, being $P(f)$ the Fourier transform of $p(t)$. Hence, using a filter whose amplitude response approximates $\cos\pi fT$ at least in the Nyquist bandwidth $|f| \leq R_b/2$, we could resort to the method in Fig. 6b. This takes care of the $T/2$ delay issue thanks to the omission of the $e^{-j\pi fT}$ factor. However, now $g_2 = \frac{1}{2}\beta g_1$, due to the omission of the factor 2 and under the hypothesis of using a filter with unit DC gain. The required cosine shape can be approximated by choosing a filter whose bandwidth B is in the order of $R_b/4$ [29]. The kind of filter is not of primary importance, even though a filter with an almost Gaussian shape (such as a Bessel-type filter) gives best results. Anyway, this method still has a delay issue, namely the delay introduced by the filter itself, so we would be simply exchanging the $T/2$ delay issue with a filter-dependent delay one. We can avoid this problem by using the same type of filter also in the quadrature branch or, better, using a single filter as shown in Fig. 7, where also the required nested Mach-Zehnder modulator (MZM) is depicted. As will be seen, using a single filter for both components may slightly modify the value of its optimum bandwidth. We found that the optimum bandwidth depends on the amount of accumulated dispersion, although only marginally, and a bandwidth of $R_b/3$ produces good results for any fiber length. The main practical issue in the implementation of the method in Fig. 7 is related to signal addition, due to the quality of electrical couplers. However, a dedicated integrated circuit design could improve the overall performance keeping the complexity very low.

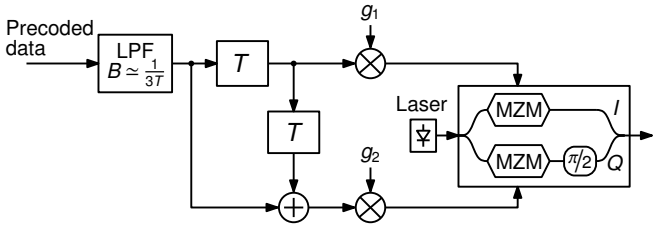

Fig. 7: IQ-duobinary transmitter.

Our approximation of a CAPS-3 signal is obtained by associating a quadrature component to a duobinary coded signal. Inspection of Fig. 7 reveals that such a component is simply given by two attenuated replicas of the duobinary signal itself, respectively anticipated and delayed by a symbol time T. For this reason we named this modulation scheme IQ-duobinary. The nested MZM's electrical drive signals for CAPS-3 (with $\alpha = 0.1$ and $\beta = 0.4$) and IQ-duobinary (with $g_2 = 0.2g_1$) normalized to the MZM V_π are shown for

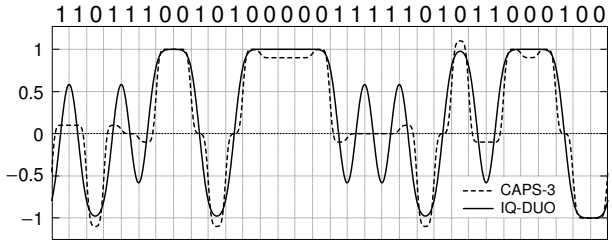

(a) In-phase drive signals.

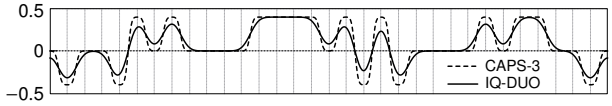

(b) Quadrature drive signals.

Fig. 8: Nested MZM electrical drive signals for CAPS-3 ($\alpha = 0.1$ and $\beta = 0.4$) and IQ-duobinary ($g_2 = 0.2g_1$) for the given binary sequence. The IQ-duobinary electrical filter is Gaussian shaped with bandwidth $R_b/3$, while a bandwidth of $0.8R_b$ was assumed for CAPS-3. The amplitudes are relative to the bias voltage and are normalized to the MZM V_π.

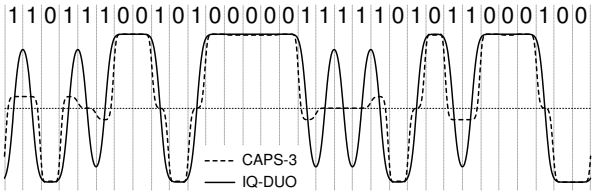

(a) In-phase components.

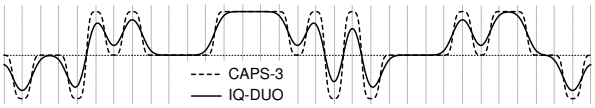

(b) Quadrature components.

Fig. 9: Electrical fields at the output of the nested MZM corresponding to the drive signals in Fig. 8. The MZM is taken to have infinite extinction ratio.

comparison in Fig. 8, while the corresponding output electrical fields are reported in Fig. 9. Looking at this last figure, it is interesting to notice that the IQ-duobinary in-phase component approximates an order-1 CAPS code, as the low signal levels are "fat" with a phase-shift in the middle [25]. However, the ratio between the maximum amplitudes of low and high levels is about 0.8, which is somewhat higher than the optimum value of 0.5, so that narrow filtered DBPSK allows a better approximation [27].[5]

[5]In the literature, there has always been a bit of confusion about what a duobinary signal is. According to a "by the book" definition, a duobinary signal is the in-phase component in Fig. 6a, while the in-phase component in Fig. 6b is only an approximation. However, this approximation is most commonly referred to as it itself being a duobinary signal. We think that it has to be also considered as an approximation to different formats such as PSBT or CAPS-1. We cannot say how much closer to a PSBT signal it is, given its loose definition [24], but we can say how much better it approximates CAPS-1. So, in the case of chromatic dispersion limited transmission, comparing the performance of CAPS-1 and the "by the book" (ideal) duobinary we find that the first one is the best of the two, whereas the latter is only marginally better than OOK [25]. The performance of what is commonly referred to as duobinary lies in between the two.

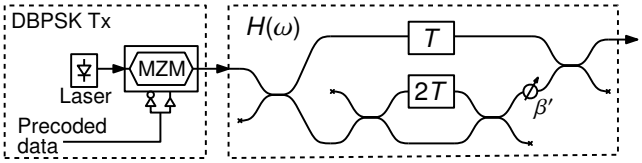

Fig. 10: IQ-DBPSK transmitter.

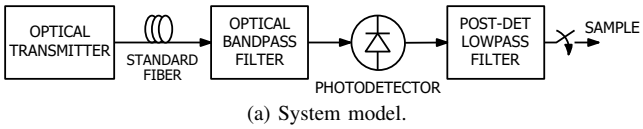

(a) System model.

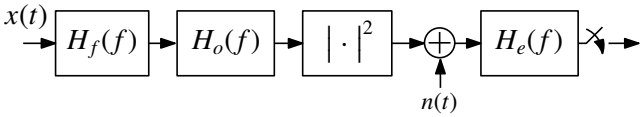

(b) Lowpass equivalent model.

Fig. 11: Block-diagram of a direct-detection optical system.

The previous observation suggests that we can also try to approximate a CAPS-3 signal by properly filtering a DBPSK signal in the optical domain, as shown in Fig. 10,[6] where the optical filter has transfer function

$$H(\omega) = \tfrac{1}{2}e^{-j\omega T} + j\tfrac{1}{4}\beta'(1 + e^{-j2\omega T}) \tag{8}$$

and could also be employed at the receiver side, instead of the transmitter one. However, such kind of filtering is difficult to realize in the optical domain. For example, in an integrated silicon photonics implementation, the necessary delays would require too long waveguides with too large losses. For this reason we will not investigate further this possible realization here, even though it would be able to provide a slightly better performance when properly adjusting the attenuation parameter β'.[7]

IV. BER Performance

The system model used for performance evaluation is depicted in Fig. 11a. The generated optical signal is launched in a standard single mode fiber and at the receiver end it is optically filtered prior photodetection. The optical filter models the operation of an optical demultiplexer that extracts the desired channel from a DWDM signal. The photodetector and the following electronic circuitry will add shot and thermal noise, respectively. The detected signal is then lowpass filtered and sampled. The only impairments taken into account will be the intersymbol-interference due to finite bandwidth of electro-optic components and chromatic dispersion, and receiver thermal noise, which is assumed to be dominant over shot noise. Hence, the lowpass equivalent model in Fig. 11b can be used, where $x(t)$, $H_f(f)$, and $H_o(f)$ are the (lowpass equivalent) transmitted optical signal, fiber frequency response,

[6]The generated optical signal has also to be filtered by a narrowband optical filter which is not shown.

[7]It must be noted that in this case the filter $H(\omega)$ would be able to approximate the inverse of the fiber transfer function, and thus not strictly a CAPS-3 signal.

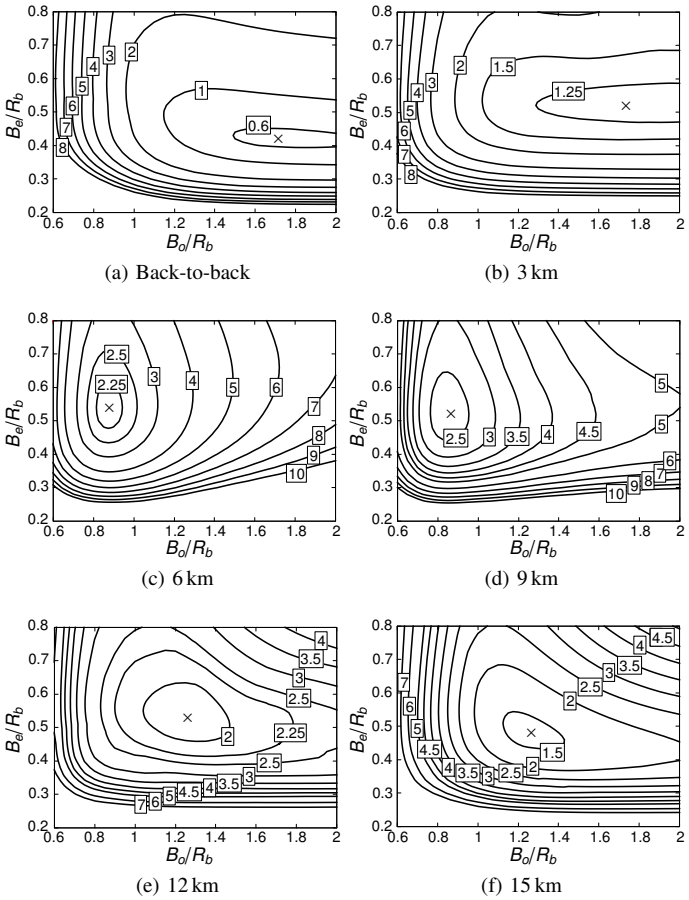

(a) Back-to-back (b) 3 km (c) 6 km (d) 9 km (e) 12 km (f) 15 km

Fig. 12: CAPS-3 contour plots of E_b/N_0 penalty at BER $= 10^{-3}$ vs electrical (B_e) and optical (B_o) filter bandwidths for six fiber lengths (reference is the performance of an OOK system in back-to-back configuration).

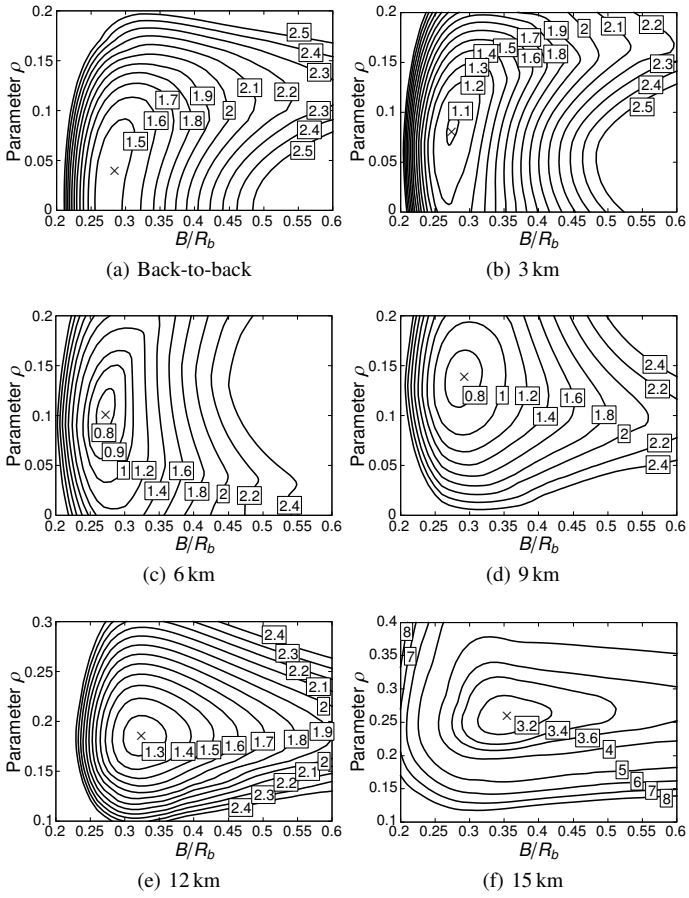

(a) Back-to-back (b) 3 km (c) 6 km (d) 9 km (e) 12 km (f) 15 km

Fig. 13: IQ-duobinary contour plots of E_b/N_0 penalty at BER $= 10^{-3}$ vs $\rho = g_2/g_1$ and the bandwidth B of the electrical filter at the transmitter (same fiber lengths and reference as in Fig. 12).

and transfer function of the optical filter, respectively, while $H_e(f)$ is the transfer function of the post-detection electrical filter modeling the response of the electronic circuitry. The thermal noise $n(t)$ is modeled as additive, white and Gaussian with monolateral power spectral density N_0. The electrical performance will be given in terms of the ratio E_b/N_0, E_b being the average electrical energy per bit. Thus, denoting by B_n the noise-equivalent bandwidth of $H_e(f)$, the corresponding signal-to-noise ratio is $\mathrm{SNR} = (E_b/N_0)R_b/B_n$. All results will be given for a standard single mode fiber with chromatic dispersion parameter $\beta_2 = -20\,\mathrm{ps}^2/\mathrm{km}$ and MZMs with an optical extinction ratio of 25 dB. A fixed bit rate of $R_b = 50\,\mathrm{Gb/s}$ is used for all considered formats and a de Bruijn sequence of suitable length adopted (2^{11} for the binary formats and 4^5 for PAM-4).[8] The electrical E_b/N_0 penalty is referred to a BER target of 10^{-3}, taking as a reference an OOK system in a back-to-back configuration. In all cases, the optical and electrical filters were considered to be 2nd- and 1st-order Gaussian, respectively. For OOK and PAM-4, the optimum $-3\,\mathrm{dB}$ bandwidths of these filters, denoted as B_o and B_e,[9] turned out to be loosely dependent on the accumulated dispersion, the optimum B_e slightly increasing while the optimum B_o slightly decreasing with increasing dispersion.

A contour plot of the E_b/N_0 penalty at BER $= 10^{-3}$ as a function of B_o and B_e can be found in [22] for OOK and PAM-4, while Fig. 12 reports the results for an actual CAPS-3 code with $\alpha = 0.1$ and $\beta = 0.4$ for six fiber lengths. In this case, while the optimum B_e turns out to be almost independent of dispersion, the optimum B_o first decreases with increasing dispersion and then increases again but only slightly. Anyway, the value of both bandwidths is not critical, as can be seen from Fig. 12. According to these findings, whatever the amount of accumulated dispersion, in the following $B_o \approx R_b$ and $B_e \approx R_b/2$ will be assumed for both CAPS-3 and IQ-duobinary, as the latter approximates the former. In this way, the E_b/N_0 penalty with respect to the optimum bandwidths is always less than about $0.5\,\mathrm{dB}$ for distances greater than $3\,\mathrm{km}$. As regards IQ-duobinary, given this choice we only have to select proper values for the ratio $\rho \triangleq g_2/g_1$ and the bandwidth B of the lowpass filter in Fig. 7. As already

[8]These values were determined by increasing the sequence length until no significant change was observed compared to the previous run.

[9]Thus, the bandwidth of the lowpass equivalent filter $H_o(f)$ is $B_o/2$.

mentioned, the type of the employed filter is not of paramount importance, although phase linearity is a desirable property. No significant difference was found using either Gaussian or Bessel-like filters, including some commercially available filters. Hence, we report here only the results obtained with a Gaussian filter. Fig. 13 shows the contour plots of the E_b/N_0 penalty at BER $= 10^{-3}$ vs ρ and B for the same fiber lengths as in Fig. 12.

As can be seen, the optimum range for B is $0.25R_b < B < 0.3R_b$ until about 9 km, and $B > 0.3R_b$ for higher distances. However, choosing a value slightly larger than the optimum produces only a negligible penalty. So, choosing $B = R_b/3$ allows for best results at higher distances (larger accumulated dispersion) while keeping the penalty within about 0.3 dB for shorter ones (smaller accumulated dispersion). As regards parameter ρ, in order to maintain the penalty within 0.3 dB, it must be chosen not larger than 0.1 until about 9 km, and then increased for larger distances. Taking an OOK system in back-to-back configuration as a reference, both electrical and optical penalties are reported in Fig. 14 for IQ-duobinary with three different values of parameter ρ and for an actual CAPS-3 code with two different choices for parameters α and β. For comparison, also the penalties of the reference OOK and a PAM-4 system are reported in the same figure. For these latter formats, the optimum bandwidths for a fiber length of 6 km were used [22].

It can be seen that IQ-duobinary performs even better than CAPS-3 for fiber lengths in the range from 5 to 10 km, but the latter fares better for larger distances. Indeed, for a given penalty CAPS-3 allows to bridge about 3 km more than IQ-duobinary. Finally, Fig. 14b shows that, allowing for a 4 dB optical power penalty with respect to OOK, PAM-4 allows to bridge about 11 km, while IQ-duobinary almost 18 km. However, PAM-4 is a multilevel signal and thus allows for a better spectral efficiency and for half the electronics speed required by IQ-duobinary, although it also requires a DAC at the transmitter and an ADC at the receiver, which are the dominant source of power consumption. Instead, as regards power consumption, both CAPS-3 and IQ-duobinary are equivalent to OOK at the receiver side, because exactly the same receiver can be used for all these last three schemes. As regards the transmitter side, the in-phase component for CAPS-3 and IQ-duobinary requires the same electrical power as OOK, while the power required by the quadrature component can be considered almost negligible, its amplitude being about 10% of the in-phase one. However, CAPS-3 requires a DAC while IQ-duobinary does not, such that it is almost equivalent to OOK also in this case.

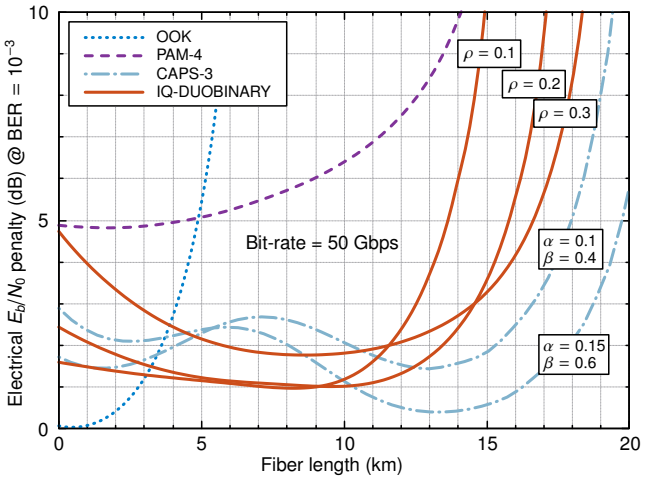

(a) Electrical penalty

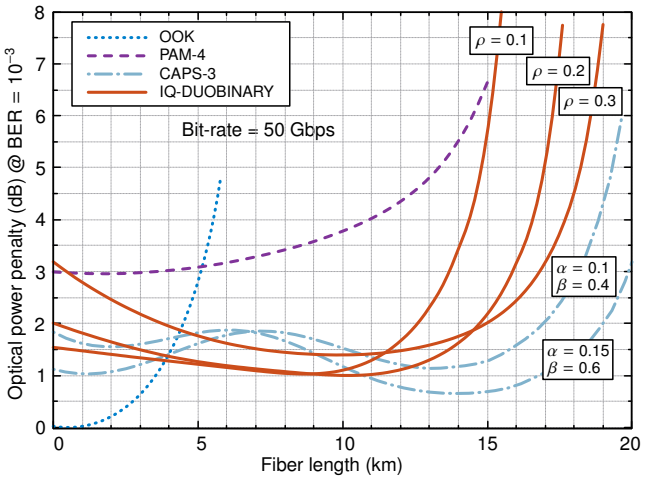

(b) Optical penalty

Fig. 14: Penalty vs fiber length.

V. Discussion and Conclusions

In short-reach optical interconnects up to 20 km, optical amplification can be avoided and direct detection is employed for cost effectiveness. In this scenario, chromatic dispersion is the main impairment and, with the constraint of avoiding DSP, only multilevel PAM formats are able to bridge this distance, seemingly. However, given a bit rate of 50 Gb/s, PAM-4 can only bridge about 11 km when accepting an optical power penalty of 4 dB with respect to a back-to-back OOK system. The distance could be increased to about 15 km but with a further 3 dB penalty. On the other hand, increasing the modulation order does not help with optical power link budget. Indeed, at least PAM-8 would be required to achieve a reach of 20 km but still requiring about 7 dB more optical power with respect to OOK [22]. Moreover, while PAM-4 is practical as a solution, PAM-8 is not because of its higher susceptibility to transmission impairments [19].

As shown here, a possible alternative to PAM is using CAPS codes for combating chromatic dispersion. Given a 3 dB penalty with respect to back-to-back OOK, a CAPS-3 code operating at a bit rate of 50 Gb/s is able to bridge 20 km at the cost of using a complex transmitter but still using the simplest direct detection receiver. By significantly simplifying the transmitter, the IQ-duobinary format allows bridging 17 km for the same penalty without requiring additional DSP. Although PAM-4 at 50 Gb/s (i.e., at 25 Gbaud) is being considered for a two-wavelength 100 Gb/s channel solution, in applications with reach significantly greater than 10 km it would require digital equalization [8], [10], [30]. In this regard, we would like to point out that, as chromatic

dispersion introduces severe nonlinear distortion to the signal due to the square-law photodetection, electronic equalization cannot be really effective unless special techniques—ruled out for short-reach applications due to their complexity—are employed [31]. In any case, the use of electronic (or optical) equalization would provide similar benefits to any modulation scheme.

In this paper, taking into account a reasonable optical power penalty (say not greater than 4 dB compared to a back-to-back OOK), a possible DSP-free alternative for bridging distances up to about 18 km at 50 Gb/s with a single-wavelength solution or at 100 Gb/s using two wavelengths has been proposed. While the transmitter is slightly more complex than for PAM-4, neither a DAC nor an ADC are necessary, and the receiver is very simple.

REFERENCES

[1] C. Kachris, K. Kanonakis, and I. Tomkos, "Optical interconnection networks in data centers: Recent trends and future challenges," *IEEE Commun. Mag.*, vol. 51, no. 9, pp. 39–45, Sep. 2013.

[2] J. L. Wei, D. G. Cunningham, R. V. Penty, and I. H. White, "Study of 100 Gigabit ethernet using carrierless amplitude/phase modulation and optical OFDM," *J. Lightw. Technol.*, vol. 31, no. 9, pp. 1367–1373, May 2013.

[3] J. D. Ingham, R. V. Penty, and I. H. White, "Orthogonal multipulse modulation in optical data communications," in *Proc. Int. Conf. Transport Optical Networks*, Cartagena, Spain, 2013.

[4] C. Ferrari *et al.*, "Compact hybrid-integrated 400 Gbit/s WDM receiver for short-reach optical interconnect in datacenters," in *Proc. Europ. Conf. Optical Commun. (ECOC)*, Cannes, France, Sep. 2014, paper Mo.4.5.2.

[5] M. I. Olmedo *et al.*, "Multiband carrierless amplitude phase modulation for high capacity optical data links," *J. Lightw. Technol.*, vol. 32, no. 4, pp. 798–804, 2014.

[6] W. A. Ling, I. Lyubomirsky, and O. Solgaard, "Digital quadrature amplitude modulation with optimized non-rectangular constellations for 100 Gb/s transmission by a directly-modulated laser," *Opt. Exp.*, vol. 22, no. 9, pp. 10 844–10 857, 2014.

[7] J. L. Wei, Q. Cheng, R. V. Penty, I. H. White, and D. G. Cunningham, "400 gigabit ethernet using advanced modulation formats: Performance, complexity, and power dissipation," *IEEE Commun. Mag.*, vol. 53, no. 2, pp. 182–189, Feb. 2015.

[8] X. Xu *et al.*, "Advanced modulation formats for 400-Gbps short-reach optical inter-connection," *Opt. Exp.*, vol. 23, no. 1, pp. 492–500, 2015.

[9] K. Zhong *et al.*, "Experimental study of PAM-4, CAP-16, and DMT for 100 Gb/s short reach optical transmission systems," *Opt. Exp.*, vol. 23, no. 2, pp. 1176–1189, 2015.

[10] Q. Hu, D. Che, Y. Wang, and W. Shieh, "Advanced modulation formats for high-performance short-reach optical interconnects," *Opt. Exp.*, vol. 23, no. 3, pp. 3245–3259, 2015.

[11] M. Sharif, J. K. Perin, and J. M. Kahn, "Modulation schemes for single-laser 100 Gb/s links: Single-carrier," *J. Lightw. Technol.*, vol. 33, no. 20, pp. 4268–4277, 2015.

[12] M. Pantouvaki *et al.*, "50Gb/s silicon photonics platform for short-reach optical interconnects," in *Proc. Optical Fiber Commun. Conf. (OFC)*, Los Angeles, CA, USA, Mar. 2016, paper Th4H.4.

[13] E. Agrell *et al.*, "Roadmap of optical communications," *J. Optics*, vol. 18, no. 6, p. 063002, 2016. [Online]. Available: http://stacks.iop.org/2040-8986/18/i=6/a=063002

[14] T. J. Xia *et al.*, "Multi-rate (111-Gb/s, 2x43-Gb/s, and 8x10.7-Gb/s) transmission at 50-GHz channel spacing over 1040-km field-deployed fiber," in *Proc. Europ. Conf. Optical Commun. (ECOC)*, Brussels, Belgium, Sep. 2008, paper Th.2.E.2.

[15] J.-X. Cai *et al.*, "20 Tbit/s transmission over 6860 km with sub-Nyquist channel spacing," *J. Lightw. Technol.*, vol. 30, no. 4, pp. 651–657, Feb. 15 2012.

[16] L. Potì *et al.*, "Casting 1 Tb/s DP-QPSK communication into 200 GHz bandwidth," in *Proc. Europ. Conf. Optical Commun. (ECOC)*, Amsterdam, The Netherlands, Sep. 2012, paper P4.19.

[17] M. Secondini *et al.*, "Optical time-frequency packing: Principles, design, implementation, and experimental demonstration," *J. Lightw. Technol.*, vol. 33, no. 17, pp. 3558–3570, Sept. 2015.

[18] C. Cole, I. Lyubomirsky, A. Ghiasi, and V. Telang, "Higher-order modulation for client optics," *IEEE Commun. Mag.*, vol. 51, no. 3, pp. 50–57, Mar. 2013.

[19] A. Ghiasi and B. Welch, "Investigation of 100GbE based on PAM-4 and PAM-8," in *IEEE P802.3bm 40 Gb/s and 100 Gb/s Fiber Optic Task Force Interim Meeting*, 2012.

[20] J. Y. Huh, J. K. Lee, S.-K. Kang, and J. C. Lee, "Analysis of PAM-N (N=4, 5, 6, 7 and 8) signals operating at 103.125 Gbps for next-generation Ethernet," in *Proc. Int. Conf. Optical Internet (COIN)*, Jeju, South Korea, Aug. 2014, paper FB4-2.

[21] R. A. Griffin and A. C. Carter, "Optical differential quadrature phaseshift key (oDQPSK) for high capacity optical transmission," in *Proc. Optical Fiber Commun. Conf. (OFC)*, Anaheim, CA, USA, Mar. 2002, pp. 367–368, paper FD6.

[22] L. S. Ronga, S. Jayousi, E. Forestieri, M. Secondini, and F. Cavaliere, "Modulation formats analysis for optical short reach interconnects," in *Proc. Fotonica 2016*, Rome, Italy, Jun. 2016, paper no. 114.

[23] S. Walklin and J. Conradi, "Multilevel signaling for increasing the reach of 10 Gb/s lightwave systems," *J. Lightw. Technol.*, vol. 17, no. 11, pp. 2235–2248, Nov. 1999.

[24] D. Penninckx, M. Chbat, L. Pierre, and J.-P. Thiery, "The phase-shaped binary transmission (PSBT): A new technique to transmit far beyond the chromatic dispersion limit," *IEEE Photon. Technol. Lett.*, vol. 9, no. 2, pp. 259–261, 1997.

[25] E. Forestieri and G. Prati, "Novel optical line codes tolerant to fiber chromatic dispersion," *J. Lightw. Technol.*, vol. 19, no. 11, pp. 1675–1684, Nov. 2001.

[26] M. Secondini, E. Forestieri, and G. Prati, "A theoretical comparison of robustness in combating CD and PMD in fiber-optic systems," *IEEE Photon. Technol. Letters*, vol. 19, no. 17, pp. 1283–1285, Sep. 2007.

[27] E. Forestieri and G. Prati, "Narrow filtered DPSK implements order-1 CAPS optical line coding," *IEEE Photon. Technol. Lett.*, vol. 16, no. 2, pp. 662–664, Feb. 2004.

[28] F. Fresi, G. Meloni, M. Secondini, F. Cavaliere, L. Potì, and E. Forestieri, "Short-reach distance extension through CAPS coding and DSP-free direct detection receiver," in *Proc. Europ. Conf. Optical Commun. (ECOC)*, Düsseldorf, Germany, Sep. 2016, paper Th.2.P.2.

[29] T. Ono *et al.*, "Characteristics of optical duobinary signals in terabit/s capacity, high-spectral efficiency WDM systems," *J. Lightw. Technol.*, vol. 16, no. 5, pp. 788–797, 1998.

[30] B. Teipen, N. Eiselt, A. Dochhan, H. Griesser, M. Eiselt, and J.-P. Elbers, "Investigation of PAM-4 for extending reach in data center interconnect applications," in *Proc. Int. Conf. Transparent Optical Networks (ICTON)*, 2015, paper Mo.D3.3.

[31] G. Colavolpe, T. Foggi, E. Forestieri, and G. Prati, "Multilevel optical systems with MLSD receivers insensitive to GVD and PMD," *J. Lightw. Technol.*, vol. 26, no. 10, pp. 1263–1273, 15 May 2008.